

The Heavy Photon Search beamline and its performance

N. Baltzell^a, H. Egiyan^a, C. Field^b, A. Freyberger^a, F.-X. Girod^a, M. Holtrop^d, J. Jaros^b, G. Kalicy^c, T. Maruyama^b, K. Moffeit^b, T. Nelson^b, A. Odian^b, M. Oriunno^b, R. Paremuzyan^d, S. Stepanyan^a, M. Tiefenback^a, M. Ungaro^a, H. Vance^c

^a*Thomas Jefferson National Accelerator Facility, Newport News, Virginia 23606*

^b*SLAC National Accelerator Laboratory, Menlo Park, CA 94025*

^c*Old Dominion University, Norfolk, Virginia 23529*

^d*University of New Hampshire, Department of Physics, Durham, NH 03824*

Abstract

The Heavy Photon Search (HPS) is an experiment to search for a hidden sector photon, aka a heavy photon or dark photon, in fixed target electroproduction at the Thomas Jefferson National Accelerator Facility (JLab). The HPS experiment searches for the e^+e^- decay of the heavy photon with bump hunt and detached vertex strategies using a compact, large acceptance forward spectrometer, consisting of a silicon microstrip detector (SVT) for tracking and vertexing, and PbWO_4 electromagnetic calorimeter (ECal) for energy measurement and fast triggering. To achieve large acceptance and good vertexing resolution, the first layer of silicon detectors is placed just 10 cm downstream of the target with the sensor edges only 500 μm above and below the beam. Placing the SVT in such close proximity to the beam puts stringent requirements on the beam profile and beam position stability. As part of an approved engineering run, HPS took data in 2015 and 2016 at 1.05 GeV and 2.3 GeV beam energies, respectively. This paper describes the beam line and its performance during that data taking.

Keywords: electron beam, collimator, heavy photon, silicon microstrips, electromagnetic calorimeter

1. Introduction

The Heavy Photon Search (HPS) experiment [1] at the Thomas Jefferson National Accelerator Facility is a search for a new $20 - 500 \text{ MeV}/c^2$ vector gauge boson A' (“heavy photon”, aka “dark photon” or “hidden sector photon”) in fixed target electro-production. Such a particle would couple weakly to electric charge by virtue of “kinetic mixing” [2]. Consequently A' s could be produced by electron bremsstrahlung and decay to electron/positron pairs or pairs of other charged particles. Since the expected coupling is ϵe , with $\epsilon \leq 10^{-3}$, A' production is small compared to standard QED production of e^+e^- pairs. To identify A' s above this copious trident background, HPS looks for a sharp bump in e^+e^- invariant mass and/or, depending on the mass and coupling, finite decay length. It does so with a compact 6-layer silicon vertex tracker (SVT) situated in a dipole magnetic field. A highly segmented PbWO_4 electromagnetic calorimeter (ECal) provides the trigger. Identifying a tiny signal above a large physics background requires a huge integrated luminosity. This is accumulated with the CEBAF CW beam, utilizing very fast electronics, a high rate trigger, and high data rate capability. To minimize the multiple scattering of the incident beam into the detector, HPS employs very thin target foils and relatively high ($\sim 100\text{s nA}$) beam currents. HPS avoids most of these scattered beam electrons as well as those that have radiated and been bent in the horizontal plane by the dipole magnet, by splitting the SVT and ECal vertically into top and bottom sections, situated just above and below the beam. The beam is passed through the entire apparatus in vacuum to minimize beam gas backgrounds.

The kinematics of the reaction are such that A' s are produced at very forward angles with energy approximately that of the incident beam ($1 - 6 \text{ GeV}$ for HPS). For A' masses of interest, the A' decay products are very forward peaked, so the detectors must be placed as close to the beam as possible. Similarly, good vertex resolution requires the silicon tracker to be as close as possible to the target. The HPS detector accepts vertical scattering angles greater than 15 mrad . The first silicon layer is positioned 10 cm downstream of the target, so the physical edge of the silicon sensor is placed just $500 \mu\text{m}$ above and below the beam (the sensor has a 1mm wide guard ring). Proximity to the beam imposes stringent requirements on acceptable beam size, stability, and halo; necessitates protection collimation; and demands real time monitoring and circuitry to protect against errant beam motion. The innermost silicon detectors see high but tolerable radiation levels and

38 roughly 1% strip occupancies close to the beam. The innermost ECal crystals
39 see roughly 1 MHz rates.

40 This paper will discuss HPS's beam requirements, the design of the HPS
41 beamline, and its performance. It will review the beamline instrumentation
42 used to measure and monitor performance and to protect against errant
43 beam motion. The excellent quality and stability of the CEBAF beams
44 coupled with HPS protection systems lets HPS take data safely with its
45 silicon detectors just 500 μm from the electron beam.

46 2. HPS Beamline

47 Fig. 1 shows the downstream end of the beam line in experimental Hall
48 B, where the HPS setup is located in the alcove downstream of the CLAS
49 spectrometer [3]. The HPS setup is a forward spectrometer based on a dipole
50 magnet, 18D36 (pole length 91.44 cm, max-field of 1.5 T) as shown in Fig.
51 2. The target and SVT are installed inside a large vacuum chamber within
52 the gap of the dipole magnet. The calorimeter (ECal) is mounted behind
53 the magnet, 134 cm downstream of the target, and split above and below a
54 vacuum chamber that connects the SVT vacuum chamber to the downstream
55 beam line and the beam dump. The ECal vacuum chamber was designed to
56 allow the innermost ECal crystals to be mounted just 20 mm from the beam
57 plane. It has two wider openings, one to accommodate most of the multiple
58 scattered beam electrons and the other, the bremsstrahlung photons created
59 in the target.

60 In order to transport the electron beam to the beam dump, two small
61 dipole magnets (pole length 50 cm, max-field 1.2 T) have been installed up-
62 stream and downstream of the spectrometer, forming a three magnet chicane
63 with zero net integrated field along the beam path. The electron beam is
64 deflected to beam's left in the first chicane dipole. It impinges on the target,
65 which is located at the upstream edge of the spectrometer magnet, 6.8 cm
66 to the left and at a horizontal angle of 31 mrad with respect to the original
67 beam line. The bremsstrahlung photon beam generated in the target contin-
68 ues in that direction after the target, while the electron beam is bent back
69 by the spectrometer magnet toward the second small dipole, which in turn
70 restores the beam to its original direction in line with the dump. Behind
71 the chicane there are two shielding walls that separate the HPS setup from
72 the downstream tunnel. A photon beam dump (a lead cave with a tungsten
73 insert) was installed after the first shielding wall, ~ 7 meters downstream of

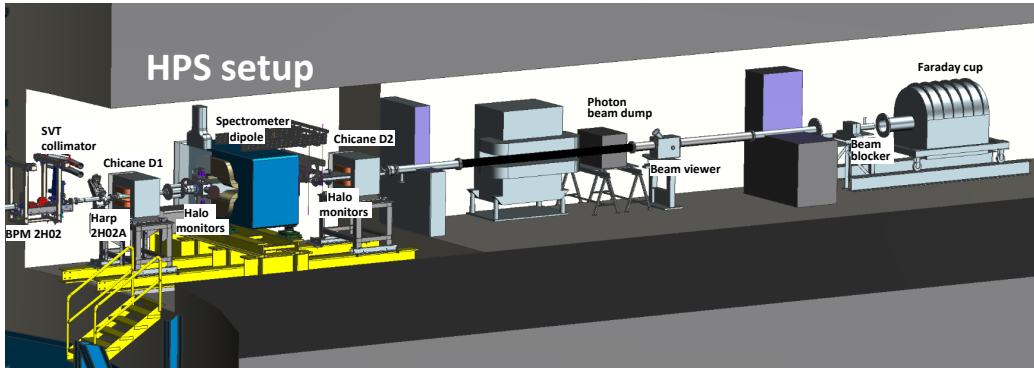


Figure 1: The 2H beam line with the HPS setup.

74 HPS. A Faraday cup cage and the Hall B electron beam dump are behind
 75 the second shielding wall.

76 The HPS experiment will run with beam energies from 1 GeV to 6.6 GeV,
 77 and beam currents up to 500 nA using 0.125% (0.25%) radiation length (for
 78 high energy runs) tungsten foils as targets. The beam parameters required
 79 to run the SVT and ECal in close proximity to the beam plane have been
 80 established using simulation and are presented in Table 1. Requiring a small
 81 beam spot improves mass and vertex resolution when beam position con-
 82 straints are included in the track and vertex fits. The tracking resolution at
 83 the target, which is much better in the vertical than horizontal direction, is
 84 reflected in the disparate beam size requirements in x and y. A small vertical
 85 beam size is also important for keeping beam tails away from the Layer 1
 86 silicon sensors.

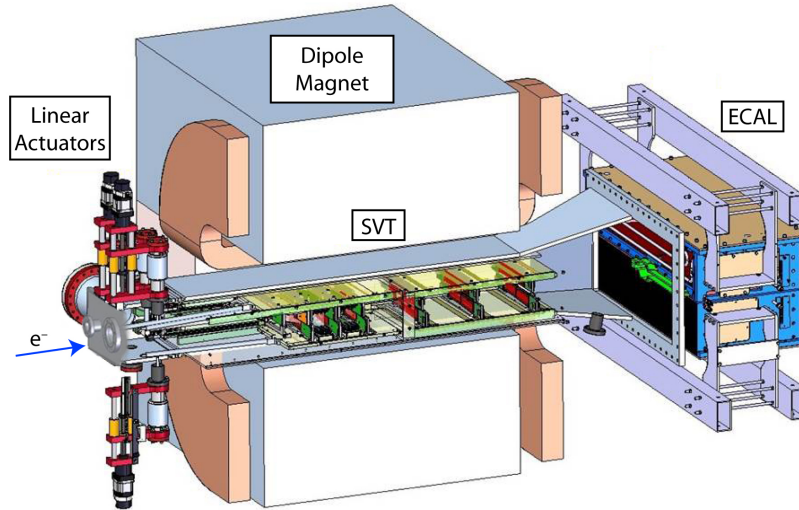


Figure 2: Partial cut-out view of the HPS setup.

87 The Hall B beamline is well equipped to deliver high quality beams and
 88 meet these requirements. Small, stable beams have been routinely delivered
 89 for experiments in Hall B [4] using the CLAS detector [3] where targets are
 90 positioned at the center of the experimental hall.

91 *2.1. Description of the Hall-B beamline*

92 The Hall B beamline is divided into two segments, the so called “2C”
 93 line, from the Beam Switch Yard (BSY) to the hall proper, and the “2H”
 94 line from the upstream end of the experimental hall to the beam dump in the
 95 downstream tunnel. The “2C” part of the beamline features an achromatic
 96 double bend (dogleg) that brings beam up to the hall’s beamline elevation
 97 from the BSY. For most experiments, where the targets are located upstream
 98 of the center of the hall, instrumentation on the “2C” line is sufficient to shape
 99 the beam profile and position it. The beam line instrumentation on “2H”
 100 line is then used only for monitoring beam properties.

101 As seen in Fig. 1, the HPS setup is located at the downstream end of the
 102 2H beam line. The HPS target is about 17 meters downstream of the nom-
 103 inal Hall B center. In order to deliver a small sized beam to HPS with the
 104 required position stability, an additional set of quadrupoles and corrector
 105 dipoles and new beam diagnostic elements have been added to the beam-

Parameter	Requirement	Unit
Beam Energy (E)	1 to 6.6	GeV
$\delta E/E$	$< 10^{-4}$	
Beam Current	50 to 500	nA
Current Stability	~ 5	%
σ_x	< 300	μm
σ_y	< 50	μm
Position Stability	< 30	μm
Divergence	< 100	μrad
Beam Halo ($> 5\sigma$)	$< 10^{-5}$	

Table 1: Required beam parameters.

106 line. This design was optimized using the beam transport software package
107 ELEGANT [5]. The beamline optimizations have incorporated the 12 GeV
108 CEBAF machine parameters and targeted the HPS beam size requirements.
109 The whole framework has been validated experimentally using the 6 GeV
110 CEBAF [6]. The optimization was done for three beam energies, 1.1 GeV,
111 2.2 GeV, and 6.6 GeV. A two-quadrupole girder based on the existing design
112 of the CEBAF arc recombiner can deliver the desired beams when the girder
113 is placed about 12 meters upstream of the hall center.

114 The devices which are actively used to control the beam in the hall and
115 monitored by the experiment are listed in Table 2. The list starts from the
116 shielding wall that separates the BSY and the Hall B upstream tunnel (this
117 is where the beam gets to the Hall B beamline elevation). The first column
118 in the table is the description of the element and the name used to identify
119 it, and the second column gives its position relative to the geometrical center
120 of the hall. The critical elements for shaping the beam profile on the HPS
121 target are the two quadrupoles on the 2H00 girder. The required beam
122 position stability was achieved by feeding back the readings of two stripline
123 Beam Position Monitors (BPM) [7], 2H00 and 2H02, to control the horizontal
124 and vertical correctors on the 2H00 girder.

125 The beam profile and position are routinely measured by the wire scanner
126 “harp”s located strategically along the beam line. In particular, the wire harp
127 “2H02A” (shown in Fig. 3), located only 2.2 m upstream of the target, played
128 an important role in confirming the beam profile and position required for the
129 experiment. This harp measures the beam profile and its projected position

Table 2: List of elements on Hall-B line from beginning of upstream tunnel to Faraday cup in downstream beam dump that are actively monitored and controlled by the experiment.

Description and section	L (meters)
Stripline BPM, quadrupoles, H/V-correctors and viewer 2C21	-40.2
Wire Harp 2C21	-38.8
nA-BPM 2C21A	-37.6
Stripline BPM, quadrupoles, and H/V-correctors, 2C22 and 2C23	-26.55 -26.5
Quadrupoles, H/V-correctors and viewer 2C24	-25.
nA-BPM 2C24A	-24.5
Wire Harp 2C24	-22.0
Hall-B tagger dipole	-17.6
Stripline BPM 2H00	-12.3
Quadrupoles and H/V-correctors 2H00	-11.6
nA-BPM 2H01	-8.0
Center of the hall	0
Stripline BPM 2H02	13.5
SVT collimator	14.1
Wire harp 2H02A	14.8
Chicane dipole 1	15.3
HPS target	17.0
Spectrometer dipole	17.5
Chicane dipole 2	19.7
Beam viewer 2H04	24.0
Dump, Faraday cup	27.0

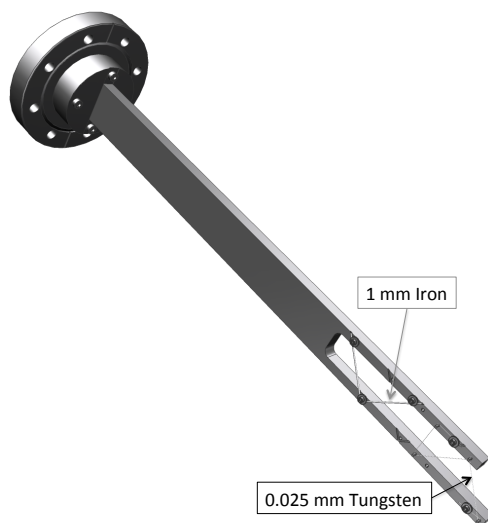


Figure 3: 2H02A Wire Harp. The thin wire is $25\ \mu\text{m}$ in diameter and the thick wire is 1 mm in diameter. The wire frame is moved into the beam at 45° .

130 along x-, y-, and 45° axes. The beam profile and position are extracted
 131 from distribution of photomultiplier (PMT) based halo monitor rates on the
 132 harp wire position while harp fork moves through the beam in 45° angle.
 133 The count rates from these halo monitors are also used as inputs to the
 134 machine fast shutdown system (FSD) as described below. In addition to the
 135 actively monitored and controlled devices, a 10 mm thick tungsten collimator
 136 was installed 3.1 meters upstream of the HPS target for SVT protection as
 137 shown in Fig. 1. It had three rectangular holes of various sizes. For most
 138 data taking during the 2016 run the $2.82\ \text{mm} \times 10\ \text{mm}$ hole was used.

139 The HPS experiment has run with beam energies of 1.05 and 2.3 GeV,
 140 and plans to run up to 6.6 GeV with beam currents up to 500 nA. The
 141 chicane magnet settings are scaled with beam energy in order to maintain
 142 the beam trajectory. HPS uses a tungsten foil target, 0.125 % of a radiation
 143 length thick at the lower energies, or 0.25 % of a radiation length at energies
 144 of 4.4 GeV or above. The foil is supported on the sides and top by a frame
 145 that has been kept very thin. This is to prevent a significant radiation dose

146 to the silicon detectors in case the beam would be accidentally deflected off
147 the target foil by, for example, an upstream magnet tripping off. The target,
148 supported on a cantilever and moved vertically by a linear actuator located
149 outside the vacuum chamber and spectrometer magnet, can be lowered on
150 to the beam line without interrupting the beam operation.

151 *2.2. SVT Mover and Wire scanner*

152 In order to bring the SVT to within 500 μm of the beam, the top and
153 bottom SVT layers 1-3 are mounted on movable support plates as shown in
154 Fig.4 Each support plate holds three sensor layers comprised of both axial
155 and stereo sensors, and a wire frame. The plate is supported by two pivots
156 on a downstream "C-support" and connected to a lever extending upstream
157 to a precision linear actuator which can move it up and down. In the nominal
158 run position, the support plates are positioned parallel to the beam and the
159 physical edge of the sensor is 0.5 mm (L1), 2.0 mm (L2), and 3.5 mm (L3)
160 from the beam. The SVT can be retracted during beam tuning or when the
161 beam is very unstable. At the fully retracted position, the layer 1 sensor
162 edge is 8 mm from the beam.

163 Also shown in Fig.4 is a beam's eye view of the bottom wire frame which
164 holds two wires and is also directly mounted on the SVT support plate.
165 The horizontal wire is 20 μm diameter gold-plated tungsten. The angled
166 wire is 30 μm diameter gold-plated tungsten and placed at 8.9 degrees to the
167 horizontal wire. While the wires are scanned across the beam using the linear
168 actuator, the downstream halo counter rates are recorded at each position.
169 Since the horizontal wire position had been surveyed in the lab with respect
170 to the nominal SVT layer 1 sensor edge with 50-100 μm precision, the SVT
171 wire scan can determine the position of the beam relative to the nominal
172 center of the SVT coordinate system. After moving the beam to the desired
173 position in the SVT coordinates, and moving the support plates to their
174 nominal positions, the silicon sensors in each of the layers are then correctly
175 positioned with respect to the beam. The distance between the horizontal
176 and angled wires is used to measure the horizontal beam position relative to
177 the SVT coordinate system with about 300 μm uncertainty. If necessary, the
178 beam is moved horizontally, so that it is properly positioned with respect to
179 the SVT.

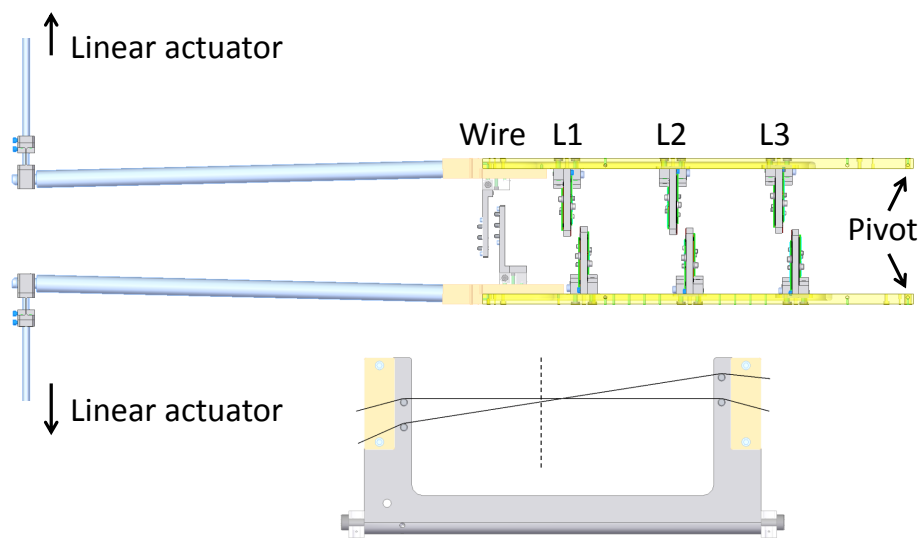


Figure 4: Elevational view of the SVT motion system and beam's eye view of the SVT wire scanner with dashed line indicating the nominal horizontal beam position.

180 **3. Beamline performance**

181 The HPS engineering runs at 1.05 and 2.3 GeV shared time in Hall B
182 with the CLAS detector upgrade project. Beams for HPS were available
183 only after regular work hours, on evenings and weekends. This arrangement
184 required re-establishing high quality beams frequently, often even daily. Such
185 operations relied heavily on the reproducibility of the beam parameters from
186 CEBAF, the stability of beamline magnet settings, the performance of beam
187 position and halo monitors, and the efficiency of beam set up procedures.

188 *3.1. Establishing beam for physics*

189 Establishing production quality electron beam for experiments in Hall B
190 is a two step process. The initial tune is done at low current by deflecting
191 the beam down to an intermediate dump with the Hall B tagged photon
192 spectrometer dipole magnet [8] and establishing the required beam profile
193 and positions using wire harps and nanoamp (nA) BPMs [9] in the upstream
194 tunnel at the 2C21 and 2C24 girders (see Table 2). An example of a beam
195 profile at 2C21 from the 2.3 GeV run is shown in Fig.5, confirming that the
196 beam was delivered to the hall with required beam profile.

197 In the second step, after degaussing and turning off the tagged photon
198 spectrometer dipole, the beam is sent straight to the electron dump at the end
199 of the Hall B beamline. Tuning and positioning the downstream beam profile
200 is done using the 3-wire harp “2H02A” mounted about 2.2 meters upstream
201 of the HPS target. An example of (X,Y) beam profile from 2.3 GeV run
202 is shown in Fig.6. Beam sizes and positions were initially measured on the
203 harp and two stripline BPMs, 2H00 and 2H02. The overall beam position
204 was then moved as needed to center the beam on the SVT coordinate system
205 using the SVT wire scanner (see above). The SVT protection collimator
206 was aligned with respect to the beam and remained inserted at all times.
207 The downstream beam viewer at 2H04, located just before a Faraday cup,
208 had three interchangeable screens, a Chromox disk, a YAG crystal, and an
209 Optical Transition Radiation foil. It was used to ensure clean beam transport
210 through the SVT collimator and the chicane and to monitor beam stability
211 during data taking.

212 After a high quality beam was established and properly aligned, the beam
213 orbit lock system was engaged. This system uses position readings from
214 the two stripline BPMs to regulate currents in the horizontal and vertical
215 corrector dipoles to minimize beam motion at the target. The response time

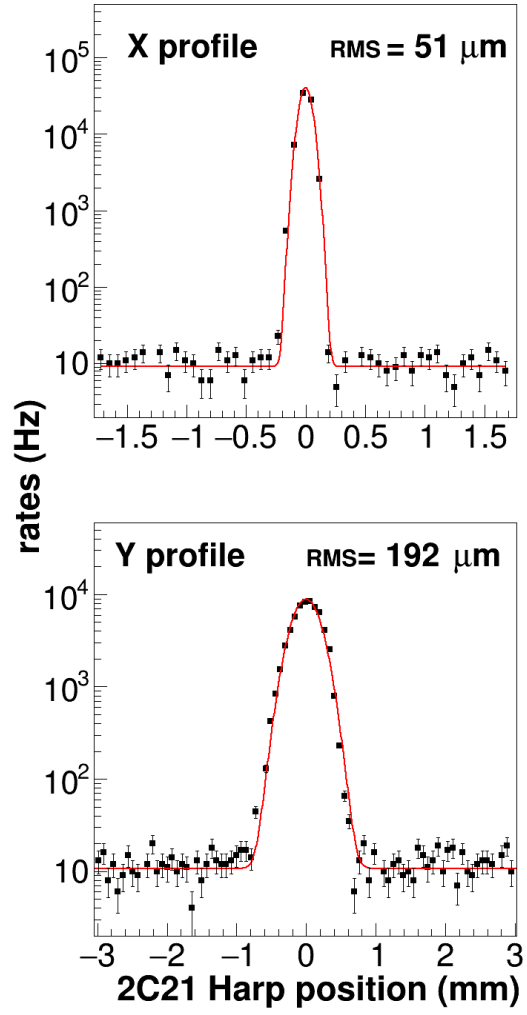


Figure 5: Beam profile measurement with wire harp 2C21.

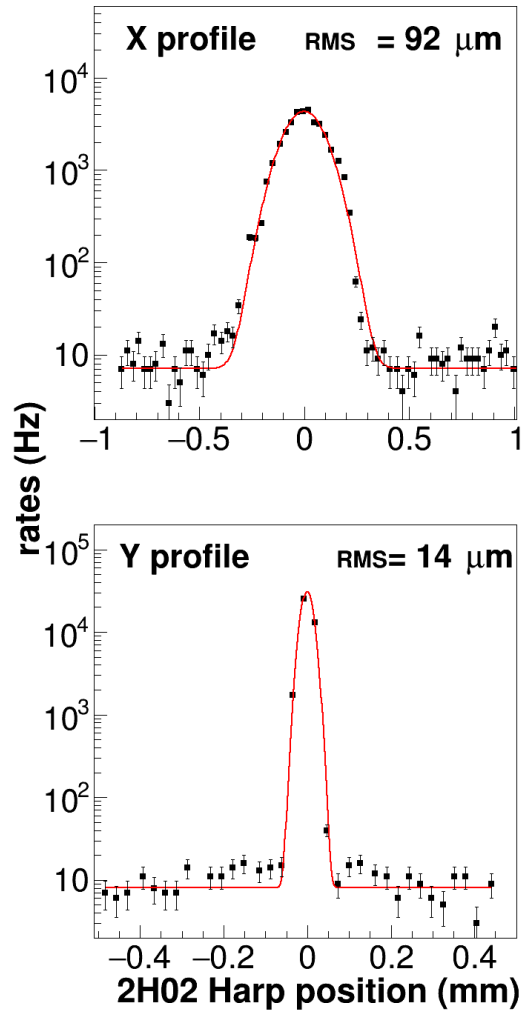


Figure 6: Beam profile measurement with wire harp 2H02A.

216 for the beam orbit corrections is of order one second and is determined by the
 217 readout bandwidth of the stripline BPMs at the operating beam currents.
 218 The position accuracy of the BPMs depends on the beam current and the
 219 readout speed. The data from the BPMs were read out and archived at a
 220 1 Hz rate. In Fig.7 the variations of (x, y) positions from the set points on
 221 these two BPMs during the entire data taking period of 2016 run are shown.
 222 The variations on the upstream BPM, labeled 2H00, are $RMS \simeq 55 \mu\text{m}$
 223 and $\simeq 84 \mu\text{m}$ for x and y positions, respectively. The variations on the
 224 downstream BPM, 2H02A, are less than $30 \mu\text{m}$ in both x and y and are
 225 within the resolution of the stripline BPMs. Similar position stability was
 226 present during the 2015 run. Based on these data and the data from harp
 227 scans where the beam profile is sampled in less than a second (the halo
 228 counter scaler readout rate is $\sim 15 \text{ Hz}$), we conclude that any beam motion
 229 at the target at less than few Hz frequency is smaller than the beam width.
 230 Based on the BPM data the vertical beam angle drift is less than $0.4 \mu\text{rad}$
 231 as the distance between the two BPMs was 25.5 meters. The observed beam
 232 angle variations have negligible impact on the beam's trajectory through the
 233 SVT.

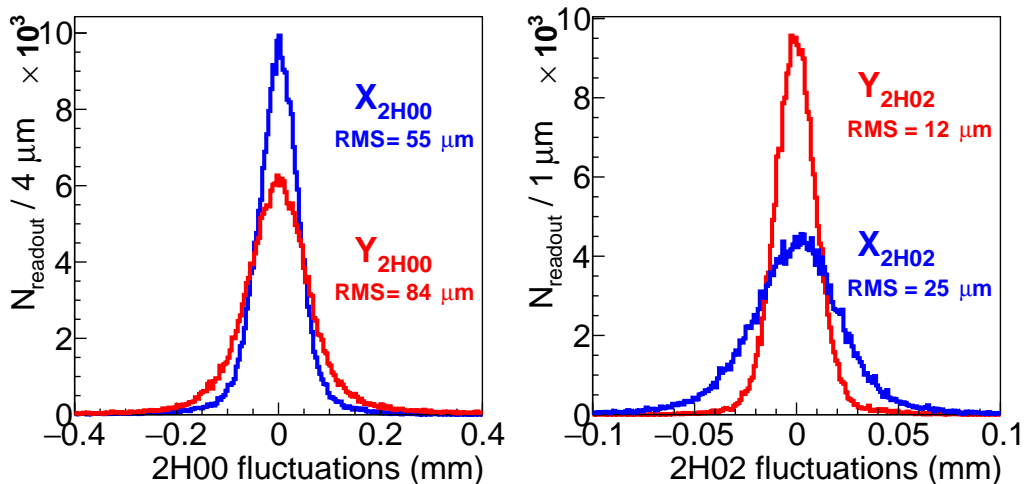


Figure 7: Distributions of beam positions at BPM 2H00 and 2H02A during the 2.3 GeV run.

234 Once a stable beam at the target is established, the chicane magnets

235 are energized and the HPS target is inserted. The final step in establishing
236 the production running conditions is setting limits on the halo counter rates
237 for the beam Fast Shut Down (FSD) system. If the beam moves close to
238 obstacles, e.g. collimator walls or silicon detector edges, count rates on the
239 beam halo monitors will increase. The threshold for the FSD trip was set on
240 the sum of the rates of the four halo monitors mounted right before and after
241 HPS target. These rates were essentially constant when beam conditions
242 were stable. Most HPS data taking took place with FSD limits set to trip
243 the beam if the sum of the halo counter rates exceeded its mean value (for a
244 fixed integration time) by 5.5σ . The integration time windows used during
245 the 2015 and 2016 runs were 5 ms and 1 ms, respectively. The trip point
246 corresponds to one false FSD trip every 16 hours if the fluctuations are purely
247 statistical.

248 While the FSD system could prevent errant beam hitting the SVT within
249 a milli-second time frame, it could not react to faster beam motions. The
250 SVT protection collimator fully protected the active region of the silicon
251 detector in Layer 1, but its protection did not extend into the 1 mm wide
252 guard ring surrounding the silicon active area and extending to within 500
253 μm of the beam. It was therefore important to understand if there is any
254 sizable beam motion at a much faster rate, outside of FSD and BPM response
255 times, that might irradiate the guard ring. A system capable of sampling
256 and storing halo monitor counts at tens of kHz rate was deployed to study
257 possible fast beam motion. This system, which was also used to test the FSD
258 system and to study beam motion during beam trips and beam restoration,
259 is described below.

260 *3.2. Beam alignment relative to SVT*

261 When the beam is delivered for the first time to HPS, or delivered after
262 a long down time, an SVT wire scan is performed to check that the beam
263 is still aligned to the SVT coordinate system. If the beam was not well-
264 aligned, it was re-centered. Fig.8 shows the halo counter rate as a function
265 of the linear actuator position for the top SVT wire scanner. The first peak
266 is from the horizontal wire and the rate difference is due to the wire size
267 difference. After fitting each peak to a Gaussian, the vertical and horizontal
268 beam positions relative to the SVT coordinate system are measured. When
269 the beam position was off more than 100 μm , the upstream corrector magnets
270 were used to move the beam, and the SVT wire scan was repeated to confirm
271 the beam movement. The wire scan shown in Fig.8 resulted in the vertical

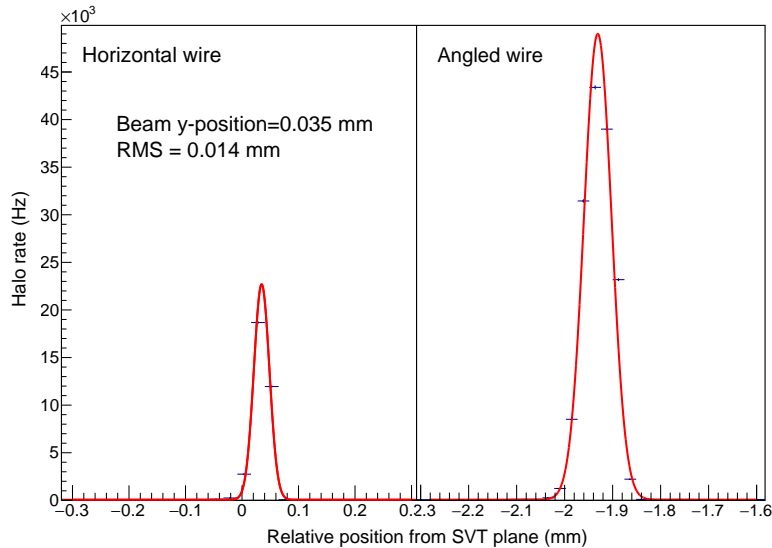


Figure 8: SVT wire scan.

272 beam position of $35 \mu\text{m}$ above and the horizontal beam position of $99 \mu\text{m}$ left
 273 of the SVT coordinate system, well within tolerances for beam placement.
 274 The vertical beam size was measured from the horizontal wire scan to be
 275 $10 \mu\text{m}$, which was consistent with the measurement by the 2H02 harp after
 276 accounting for the fact that the beam is being focused to the target location,
 277 and the harp is about 2 meters upstream. Once the beam position was
 278 established, the SVT wire scan was performed only sparingly since the orbit
 279 lock system could maintain the beam position well within $50 \mu\text{m}$.

280 3.3. Beam motion studies

281 Several studies have been done to understand beam position stability be-
 282 yond those possible with the standard control and monitoring system. Sig-
 283 nals from halo monitors downstream of the HPS target were fed to a Struck
 284 SIS3800 scaler VME module read out by EPICS Input-Output Controller
 285 (IOC) running on a Motorola MVME5500 CPU board. This application al-
 286 lowed us to latch the scalers for time intervals as short as 15 microseconds
 287 and to write them into ROOT [10] files for offline analysis. The following
 288 studies were done using this system to look for short term beam motions.

289 *3.3.1. Fast beam motion*

290 To get reasonable halo counter statistics in a 15 microsecond window,
 291 the beam must be parked close to a solid object so its tails can produce
 292 high backgrounds. For the first study, the 1 mm thick iron wire strung
 293 horizontally on 2H02A harp (Fig. 3) was positioned close to the beam core
 294 to get sufficient rates. A change of rate indicates beam motion towards or
 295 away from the wire. Both wire positions, above and below the beam,
 296 were studied, to be sensitive to possible fast beam motions in either direction.

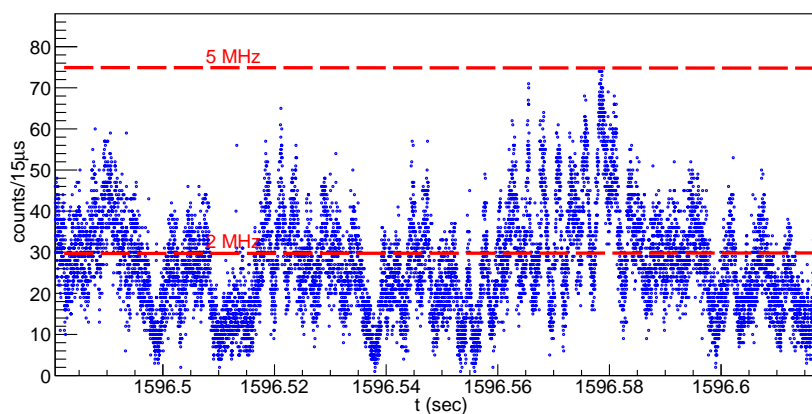


Figure 9: Oscillations of rates on HPS_SC in the 140 ms time interval.

297 Fig.9 shows a 140 ms snapshot of the scaler readout. With 100 nA
 298 beam current, the average rate was 30 counts per 15 μ s, or 2 MHz. The
 299 maximum rate was about 75 counts per 15 μ s or 5 MHz. Since such rapid
 300 rate fluctuations were not observed on the same monitors when the HPS
 301 target was inserted, the observed fluctuations are attributed to oscillations
 302 in the beam position.

303 To estimate how large these beam motions are, the same halo rates were
 304 measured every 0.1 second while the wire was passing through a 10 nA beam
 305 at a speed of 0.5 mm/sec, while the full beam vertical profile was measured.
 306 Fig.10 shows a small portion of that scan corresponding to positions between
 307 the beam and the wire at which the rate fluctuation data shown above was
 308 taken. The red line on the figure corresponds to the Gaussian fit to the beam
 309 profile. The motor positions corresponding to 2 MHz and 5 MHz count rates
 310 at 100 nA beam current (after correction for the readout speed and the beam
 311 current) are shown with blue dashed lines. The difference between these two
 312 positions, after accounting for the fact that the harp moves at 45 degrees

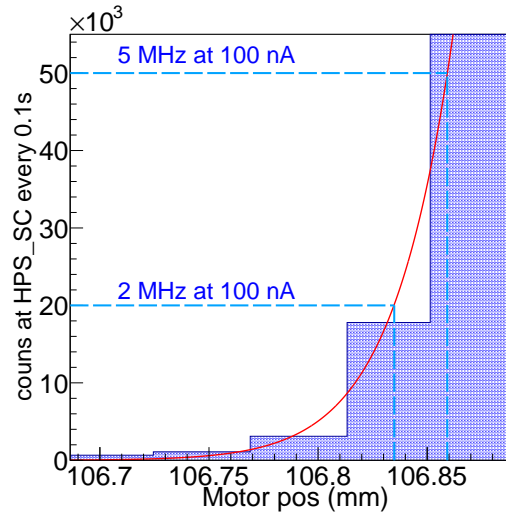


Figure 10: Counts on the halo monitors as a function of harp motor position. The red solid line is the Gaussian fit to the whole beam profile. The two blue dashed vertical lines show position of the wire where rates are 0.2 MHz and 0.5 MHz.

313 with respect to the vertical axis, is $\approx 17.7 \mu\text{m}$. So vertical beam oscillations
 314 of just $18 \mu\text{m}$ will account for the observed rate variations, and this is much
 315 smaller than the vertical beam size of $\sim 30 \mu\text{m}$. Fast beam motion is not a
 316 problem for HPS.

317 3.3.2. Beam motion during beam trips

318 There are various causes for beam trips: beam loss in the machine itself;
 319 beam loss in the delivery lines which cause rate increases on beam loss or
 320 halo monitors; RF system trips or loss of RF to an accelerating cavity. The
 321 average beam trip rates were 5 and 10 per hour during HPS runs in 2015
 322 and 2016, respectively. Depending on the cause of the trip, the beam could
 323 conceivably move vertically and hit the exposed regions of the SVT before it
 324 is shut off. The time it takes to shut the beam off is expressed as:

$$t = 27 \mu\text{s} + N_{\text{pass}} \cdot 4.2 \mu\text{s}/\text{pass} + \text{Detection time} \quad (1)$$

325 where $27 \mu\text{s}$ is the time it takes to shut the beam at the injector and
 326 $4.2 \mu\text{s}/\text{pass}$ is the time it takes to clear the machine. The “Detection Time”

327 depends on the source of the trip and can take milliseconds, e.g for the HPS
328 halo monitor FSD system that time is 1 ms. If there is a large beam motion
329 towards the SVT or other obstacles (collimator or beam pipes), this should
330 be captured in the halo monitor rates when they are read out rapidly. Us-
331 ing the Struck scaler setup a couple of dozen beam trips and beam recovery
332 periods have been recorded. There were no rate increases during the beam
333 recovery, indicating no appreciable beam motion. In 30% of the beam trips,
334 some rate increase was observed within 200 μ s prior to beam shut off. This
335 could have been due to beam motion at the SVT or to higher beam back-
336 grounds passing through the entire beam line. Our measurement does not
337 differentiate between these possibilities. Since many of these instances of
338 increased halo counter rates coincided with increased upstream halo counter
339 rates, it is likely that beam motion was not to blame in these cases.

340 3.3.3. Test of the FSD system

341 The CEBAF Fast Shut Down (FSD) system provides permissive signals
342 to the injector gun. If the permissive is removed, the gun shuts off within 27
343 μ s. The sum of the HPS halo counter rates was used for one of the inputs to
344 the FSD system.

345 After setting up production running, the halo counter rates were increased
346 by running the 2H02A harp wire through the beam, simulating the condition
347 where the beam tail is hitting an obstacle. The system was tested for 1
348 ms, 5 ms, and 10 ms integration times. In Fig.11 one of the measurements
349 with FSD integration time set to 1 ms is shown. Each point on the graph
350 is the integrated counts over 300 μ s. The red line on the graph is the trip
351 threshold, 62 counts per 300 μ s or 206 kHz. As one can see there are four
352 cases when rates go above the red line, three of which have only one point
353 (300 μ s) above the threshold. The fourth one has three points ($3 \times 300 \mu$ s)
354 above the red line after which beam tripped as one would expect for trip
355 integration time of 1 ms. The same tests with 5 ms and 10 ms integration
356 times gave consistent results.

357 3.4. Beam halo

358 HPS is very sensitive to excess beam halo. As the active area of the
359 silicon sensor at layer 1 starts at 1.5 mm, we require that any beam halo
360 extending beyond 1.5 mm do not contribute significantly to the sensor oc-
361 cupancy. Fig.12 shows the SVT axial layer 1 occupancy during 2015 data
362 taking at 50 nA and a special run without the target. The SVT protection

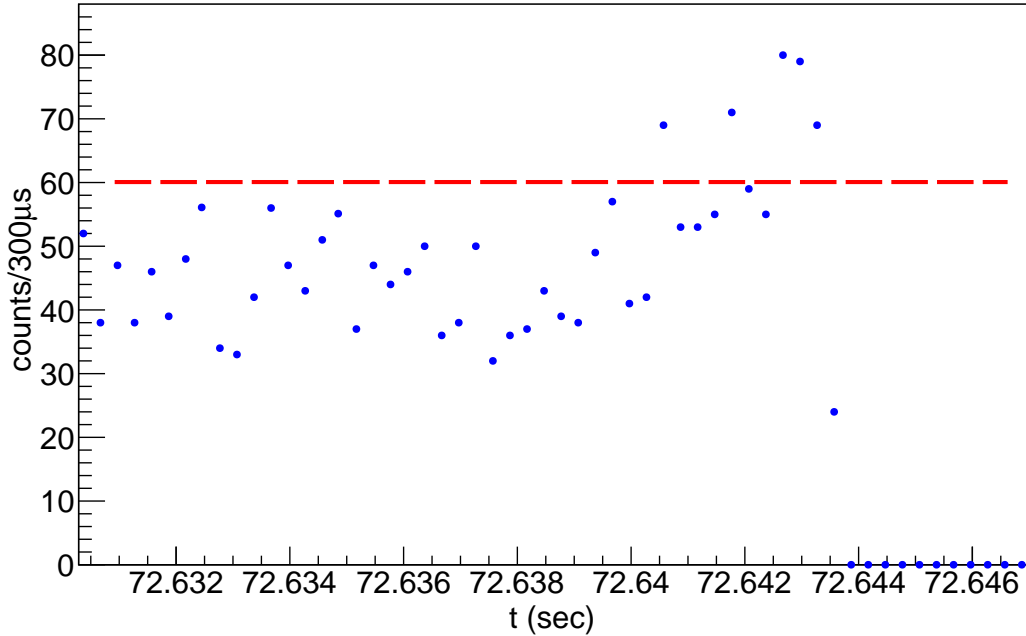


Figure 11: HPS halo counter rates as a function of time. The FSD integration time is 1 *ms* and the beam current is 200 nA. Each point represents integrated counts over a 300 μ s time interval.

363 collimator with 4 mm \times 10 mm hole was used. The 0.7 % occupancy during
 364 data taking was mostly due to Coulomb scatterings in the target and was
 365 consistent with expectation. Extra hits from the beam halo were observed
 366 in the first ten channels when the target was removed. However, the extra
 367 hits was less than 20% of the nominal occupancies. The halo was consistent
 368 with a Gaussian distribution with $\sigma = 1$ mm at the intensity level of 10^{-5}
 369 of the core beam and was consistent with the large dynamic range harp scan
 370 [4]. The sharp drop in the halo hits beyond 2 mm is due to the collimator,
 371 and no extra hits from the beam halo was observed during the 2016 run as
 372 the vertical size of the collimator hole was reduced to 2.82 mm.

373 4. Summary

374 The HPS experiment took data successfully at 1.05 GeV and 2.3 GeV
 375 beam energies with the silicon sensor edge at only 500 μ m from the beam.

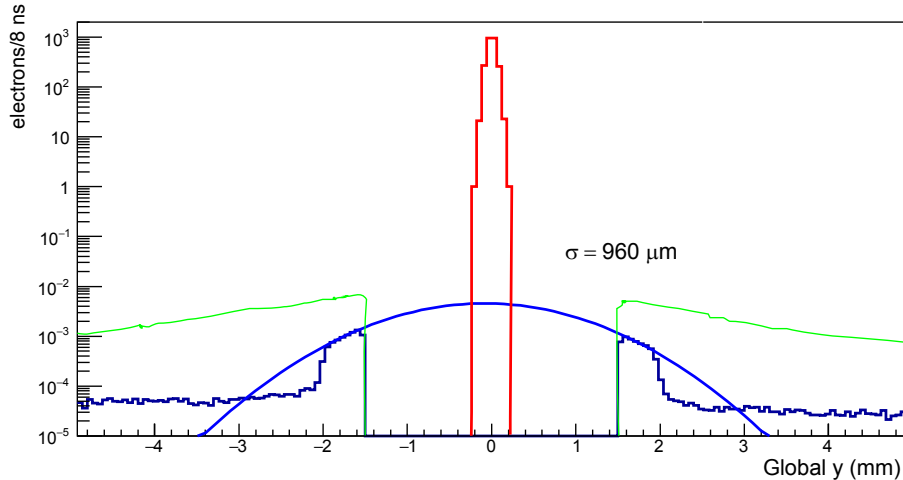


Figure 12: SVT axial layer 1 occupancy during data taking run (green) and no target run (blue). The histogram in red is nominal 50 nA Gaussian core and the blue curve is a Gaussian fit to the halo with σ of 960 μm .

376 High quality beam with very small halo was delivered and stable beam po-
 377 sition was maintained by the beam feedback system. The fast shut down
 378 system worked in protecting the silicon sensors from errant beam exposure.

379 5. Acknowledgements

380 The authors are grateful for the outstanding efforts by the staff of the
 381 Accelerator Division and the Hall B technical staff at Jefferson Lab, and for
 382 taking high quality data by the HPS collaborators. This material is based
 383 upon work supported by the U.S. Department of Energy, Office of Science,
 384 Office of Nuclear Physics under contract DE-AC05-06OR23177, and Office
 385 of High Energy Physics under contract DE-AC02-76SF00515.

386 [1] A. Grillo, et al. (HPS Collaboration), *HPS Proposal for 2014-*
 387 *2015 Run*, 2014. [http://confluence.slac.stanford.edu/download/](http://confluence.slac.stanford.edu/download/attachments/86676777/hps_2014.pdf)
 388 [attachments/86676777/hps_2014.pdf](http://confluence.slac.stanford.edu/download/attachments/86676777/hps_2014.pdf)

389 [2] B. Holdom, Phys. Lett. B 166, 196 (1986).

390 [3] B. Mecking, et al., Nucl. Inst. and Meth. A 503, 513 (2003).

- 391 [4] A. Freyberger, JLAB-ACC-05-318 (2005).
- 392 [5] M. Borland, A Flexible SDDS-Compliant Code for Accelerator Simula-
393 tion, ANL, Argonne, IL 60439, USA
- 394 [6] HPS update to PAC39,
395 https://www.jlab.org/exp_prog/proposals/12/C12-11-006.pdf
- 396 [7] P. Evtushenko, A. Buchner, H. Buttig, P. Michael, B. Wustmann, K.
397 Jordan, *Stripline BPM Monitors for ELBE*, Proc. DIPAC 2001, ESRF,
398 Grenoble, France.
- 399 [8] D. Sober et al., Nucl. Inst. and Meth. A 440, 263 (2000).
- 400 [9] M. Piller, et al., JLAB-ACC-99-30 (1998).
- 401 [10] R. Brun and F. Rademakers, *ROOT - An Object Oriented Data Analy-*
402 *sis Framework*, Proceedings AIHENP'96 Workshop, Lausanne, Septem-
403 ber 1996. <http://root.cern.ch/>